Alterations in the Function of the Ubiquitin Proteasome System in Human Cardiac Diseases and a Mouse Model of Myocardial Infarction

Frank Davis
University of Michigan 2010
Cellular and Molecular Biology Honors Thesis
PI Mentor: Dr. Sharlene Day
Honors Advisor: Professor Kenneth Cadigan

INTRODUCTION

The proteome is in a dynamic equilibrium of synthesis and degradation. Although, synthesis plays an important role in controlling the steady state concentration of some proteins, degradation pathways provide an equally important contribution to regulating protein turnover. The two major cellular degradation pathways are the lysosomes and the ubiquitin proteasome system (UPS). Lysosomes degrade mostly endocytosed membrane proteins. In contrast, the ubiquitin proteasome system is responsible for degradation of the majority of intracellular proteins (up to 80-90% of all intracellular proteins in mammalian cells) (1), which include not only damaged, misfolded, or aged proteins, but also many proteins vital to eukaryote biology such as those involved in the cell cycle and transcriptional regulation (2-4). The degradation process of the UPS is divided into two steps. First, intracellular proteins are marked for degradation through the covalent linkage of a string of ubiquitin molecules. Ubiquitin is a highly conserved 76 amino acid sequence that is linked to lysine residues of selected proteins through an enzymatic cascade involving E1 (ubiquitin-activating enzyme), E2 (ubiquitin-conjugating enzyme) and E3 (ubiquitin ligase) (5). A polyubiquitin chain is then assembled onto the targeted protein via an isopeptide linkage between the lysine residue of the previous ubiquitin and the C-terminal glycine residue of the subsequently attached ubiquitin.

The second step of the ubiquitin degradation pathway involves the 26S proteasome complex that contains the proteolytic activity that catalyzes the degradation of polyubiquitinated proteins. The 26S proteasome complex is composed of the 20S proteolytic core and the 19S activation complex, which is situated on one or both ends of the 20S proteasome (13). The 20S proteasome is a cylindrical-barrel shaped complex containing 28 subunits arranged in two α and two β rings with α1-7, β1-7, β1-7, and α1-7 symmetry (Figure 1). The proteolytic activity of the

UPS resides in three β subunits, specifically the β1, β2, and β5 subunits. In general, the three main proteolytic activities that have been ascribed to the proteasome include: caspase-like (β1), trypsin-like (β2), and chymotrypsin-like (β5) activity. Flanking the inner β core on both sides is a ring of α subunits that do not maintain any proteolytic activity. However, crystallographic structural analysis of the proteasome shows that these α subunits partially prevent substrate access to the central chamber by forming the α annulus that projects into the openings at either end of the cylinder (6-8). Despite this partial blockage, the 20S proteasome can degrade any protein that is able to enter the central chamber, however degradation remains relatively inefficient.

The inefficient degradation by the 20S proteasome is overcome when one or two 19S complexes bind on one or both sides of the 20S forming the active 26S proteasome. The 19S complex consists of 17 subunits that form two distinct subcomplexes: the base and the lid. The base is composed of six ATPase subunits (Rpt1-Rpt6) and two larger non-ATPase subunits (Rpn1and Rpn2) (Figure 1). The six ATPase subunits form a ring that sits on top of the outer α ring (6, 9). The primary functions of the base include: activating the 20S proteasome by rearranging the α annulus, hydrolyzing ATP to unfold substrate proteins so they can be translocated through the central channel of the 20S proteasome, and providing an attachment point for the 19S lid (10-11). The lid complex is composed of the remaining nine subunits of the 19S and possesses the Rpn 10 subunit which is responsible for recognition of polyubiquinated proteins and the Rpn 11 subunit that deubiquitinates substrates prior to their passage into the 20S core in an ATP dependent manner (12). Additionally, the 20S can associate with the 11S activator complex (PA28α, PA28β, and PA28γ) at one or both ends which promotes proteolytic degradation in an ubiquitin and ATP independent manner.

Even though assembly and stability of the 20S proteolytic core with the 19S or 11S provides one manner for regulation of the UPS degradation pathway, post-translational modifications also offer another level of control. Recent work by Zong et al. described novel phosphorylation patterns on the 20S complex and identified two associating partners, protein kinase A (PKA) and protein phosphatase 2A (PP2A) (14). They also showed that *in vitro* administration of PKA increased the overall proteolytic activity and increased the phosphorylation of certain 20S subunits. Additional support for the importance of PKA-mediated regulation of the proteasome was provided by Zhang et al. who showed that PKA phosphorylation of the 19S ATPase Rpt6 subunit was important for activation of the proteasome *in vitro* (13).

Besides phosphorylation, oxidation has also been shown to have an equally important effect on the UPS. The UPS is responsible for degrading most oxidized proteins, however under conditions of intense oxidative stress the accumulation of oxidized proteins overwhelm the functional capacity of the UPS resulting in the formation of insoluble oxidized protein aggregates and overall UPS impairment (32, 33). In addition, oxidative modification to the proteasome itself has been shown to inhibit proteasomal function (34). Overall, modifications including oxidation and phosphorylation have been shown to affect the stability, activity, and assembly of the 26S proteasome and provide vital dynamic responses to cell signals and stresses (9, 13-16).

Role of the 26S Proteasome in Cardiac Diseases

Dysfunction of the UPS has been well characterized in a variety of human disorders including neurodegenerative disorders, cataracts, and muscle atrophy (17-20). However,

investigations into the relationship between the UPS and cardiovascular diseases are only beginning to emerge. Previous animal studies have reported UPS dysfunction in a desmin-related cardiomyopathy through the accumulation of protein aggregates and the depletion of key components within the 19S (21). In addition, animal models of myocardial ischemia have shown increased oxidation of the proteasome resulting in decreased proteolytic activity and an increase in the cellular accumulation of ubiquitinated substrates (22, 23). Lastly, a recent study on a genetic animal model of cardiomyopathy suggested that truncation mutations in cardiac myosin binding protein C (cMyBP-C) competitively inhibit the degradation of UPS substrates and may be a contributing factor to the pathogenesis of familial hypertrophic cardiomyopathy (25). Familial hypertrophic cardiomyopathy is the most common heritable cardiovascular disease affecting 1 in 500 individuals and is primarily caused by heterozygous mutations in sarcomere genes. Hypertrophic cardiomyopathy is characterized by cardiac hypertrophy and a broad clinical spectrum that includes heart failure, arrhythmias, and sudden cardiac death. Yet overall, studies in animal models of cardiac hypertrophy are in disagreement showing both inhibition and activation of the UPS (26-28). Limited data are available on the relationship between the UPS and human cardiac hypertrophy.

The current work seeks to investigate protein degradation and turnover by the UPS in cardiac muscle diseases using both human cardiac tissue and a mouse model of myocardial infarction. The first half of the study investigates UPS activity in different human cardiac disease states: end-stage heart failure (F) and hypertrophic cardiomyopathy (HCM). We found a significant reduction in proteasomal activity in both F and HCM tissue in comparison to non-failing controls. In addition, HCM patients who carried mutations in myofilament genes had significantly lower proteasome activity compared with HCM patients lacking pathogenic

mutations. These results are particularly interesting given a previous study that showed that a HCM-associated cMyBP-C truncation mutation impaired UPS function (25). I have begun to investigate the hypothesis that cMyBP-C mutations could impair UPS activity in human tissue by altering the tight stoichiometry normally maintained by the sarcomere. I found that overall protein expression level of cMyBP-C was significantly reduced in samples containing *MYBPC3* mutations. I have also begun to study the stoichiometric ratios of mutant and wild-type MyBPC and other sarcomere proteins in human samples, with the intent to learn how mutations in these proteins affect their stability and interactions with their wild-type partners.

Finally in the second half of this study, we investigated the effects of myocardial infarction on UPS function. In contrast to what was observed in human heart tissue, we found that proteasomal activity was significantly *increased* in infarcted hearts two weeks after left coronary artery ligation. Yet, I did not observe an increase in content of subunits from the 20S core, the 19S regulatory cap, or the 11S activator. The activation of the proteasome could be explained through posttranslational modifications for which I developed an immunoprecipatation protocol coupled with LC/MS/MS analysis to analyze differential phosphorylation. My investigations show that phosphorylation of the α-7 (43), previously shown to be important to the stability of the 26S complex, was not significantly different in mice following myocardial infarction. Current research is underway to study phosphorylation differences in other proteasomal subunits following myocardial infarction.

METHODS

Human heart tissue procurement: Tissue from non-failing, failing, and HCM hearts was collected as described in Predmore et al (24). Tissue collection from human hearts used in this

study has the approval of the University of Michigan Institutional Review Board (IRB) and subjects gave informed consent.

Chemicals and reagents: Fluorogenic substrates Suc-LLVY-AMC and Z-LLE-AMC, proteasome inhibitor lactacystin, and all antibodies used to detect proteasome subunits and polyubiquinated proteins were from Biomol International (Plymouth Meeting, PA). Antibodies for rabbit and mouse GAPDH were from Abcam and Chemicon respectively. The antibody raised against the first 14 amino acids of cMyBP-C was kindly provided by Sakthivel Sadayappan. The antibody designed to recognize substrates of PKA dependent phosphorylation was acquired from Cell Signaling. ProQ Diamond phosphor stain (Molecular Probes) and SYPRO RUBY protein stain (Bio-Rad) were also used for detection of phosphorylated proteins and total protein, respectively.

Proteasome activity assay: Chymotrypsin-like and caspase-like activity of the proteasome from cardiac tissue was measured using an optimized procedure outlined by Predmore et al (24).

Immunoblotting and densitometry analysis: Protein concentration was determined by the Bradford method. Protein extracts were denatured by boiling and sonication, resolved by SDS-PAGE, transferred to nitrocellulose membranes, and blocked in 5% milk. Blots were probed with primary antibodies for 1-18 hours, followed by fluorescent-tagged secondary antibodies for 1 hour. Imaging and densitometry analyses were performed using the LI-COR Odyssey laser scanner or ImageQuant TL software and band intensity was normalized to GAPDH as a protein loading control unless otherwise specified.

Quantitative mRNA analysis: The quantification of cMyBP-C mRNAs was performed by two step RT-PCR coupled with Taqman hydrolysis probes. Total RNA was extracted from human tissue using the RNeasy kit (Qiagen) according to the manufacturer's instructions. RNA concentration, purity, and quality were determined using Biophotometer Plus (Eppendorf). RT was performed using Omniscript RT kit (Qiagen) according to manufacturer's instructions and cDNA concentration was determined by the Biophotometer Plus. A Taqman hydrolysis probe specifically recognizing the exon 2-3 junction with human cMyBP-C was used for quantification of mRNA transcripts (Applied Biosystems). β-actin was used as an endogenous referent gene. Experiments were performed on the 7000 Sequence Detection System (Applied Biosystems). The relative mRNA amount was estimated according to the comparative Ct method with the $2^{-\Delta\Delta Ct}$ formula in comparison to non-failing control samples.

Absolute Quantification of Abundance (AQUA): In collaboration with NextGen Inc., the ratio of mutant to wild type proteins in human tissue heterozygous for the cMyBP-C R495Q mutation was calculated by engineering peptides corresponding to a specific wild-type peptide sequence (DGVELTREETFK) and a specific mutant peptide sequence (DGVELTQEETFK). These AQUA peptides were synthesized with isotopically enriched Lysine containing ^{13}C and ^{15}N. Purity of both stable-isotopelabeled peptides was verified by HPLC. The masses of the isotope-labeled peptides were measure by MALDI-TOD-MS. Endogenous peptides were obtained by performing a myofilament preparation on human cardiac tissue as described in Wolff et al. (48) and separating the myofilament proteins using SDS-PAGE. The cMyBP-C band of interest was identified and gel excised. The band was digested by reducing with DTT at 60^{o}C then allowing

the solution to cool to room temperature followed by alkylation with iodoacetamide. The endogenous sample was then incubated at 37^{o}C for 4 hr in Lys-C (creating wild type and mutant peptides the same length as the synthesized peptides) and the reaction was stopped with formic acid. The supernatant was then analyzed directly. A 38µl aliquot of the supernatant was spiked with 2 µl of 10fmol/µl of AQUA peptide (to yield 0.5 fmol/µl in the sample). A 10µl injection of the sample was then analyzed on a LC chromograph with peak areas calculated using Thermo Qual Browser software. After, the ratio of peak areas for the light peptide (endogenous peptide) and heavy peptide (AQUA peptide) was calculated and exact amounts of mutant and wild type peptides determined based on the known quantity of AQUA peptide injected.

LCA Ligation Model: Heart failure in mice age 3 to 4 months was induced through permanent left coronary artery ligation performed by Dr. Sharlene Day as previously described (31). Hearts were harvested after 2 weeks, which was the time point of maximal proteasome activation.

Proteasome Immunoprecipation: Tissue homogenates were prepared in 1X RIPA buffer (Millipore) supplemented with 1nM Calyculin A, 1mM Sodium Orthovanadate, 1 mM sodium fluoride, 1 µg/mL aprotinin, 1 µg/mL leupeptin, and 1 µg/mL pepstatin and incubated at 4^{o}C for 30 minutes. The homogenates were centrifuged at 14,000xg for 10 minutes and the supernatant removed. The supernatant was pre-cleared by adding 100 µl of Protein A Sepharose beads and shaking for 1 hour at 4^{o}C. The protein concentration of the supernatant was determined using the Bradford method and then diluted to 4 µg/mL in PBS. To immunoprecipitate the proteasome, the supernatant was incubated with 2.5 µl of rabbit anti-Rpt-6 (Biomol), for purification of the 19S proteasome, or rabbit anti-α-3 (custom antibody), for purification of the

20S proteasome antibody overnight at 4^{o}C. The immunocomplex was collected by adding 100 µl of Protein A Sepharose beads to the sample and incubating for 1 hour after which the sample was centrifuged at 3000xg for 10 minutes. After removing the supernatant, the pellet was washed three times in 1X PBS. The proteasome-bound Protein A Sepharose beads were incubated in laemmli buffer for 5 minutes at 100^{o}C. The samples were centrifuged at 5000xg and the supernatant containing the proteasome was collected for analysis.

2-Dimensional Gel Analysis: For 2-Dimensional gel electrophoresis (2DE), purified 26S proteasomal complex was lyophilized from laemmli buffer and resuspended in IPG rehydration buffer. pH strips 4-10 (Bio-Rad) were rehydrated in this solution and the sample was then separated on the Bio-Rad 2D electrophoresis system. After IEF, IPG strips were reduced by 2% DTT solution and alkylated by 2.5% iodoacetic acid (IAA) sequentially for 10 minutes each. The second dimension electrophoresis was done on Bio-Rad precast Criterion gel (12.5%). The resulting 2D gel was either stained with SYPRO RUBY and used in LC/MS/MS application or transferred to nitrocellulose membrane for western blotting.

LC/MS/MS Analysis and Defining Phosphorylation of Proteasome Subunits: Enriched 26S proteasome preparations were separated by SDS-PAGE. Regions of interest were identified based on molecular weight of the proteasome and these regions were excised into seven equal segments. Each segment was digested with trypsin and analyzed using LC/MS/MS with a 1 hour gradient on the LTQ Orbitrap XL mass spectrometer. The resulting product ion data were searched against the forward and reverse IPIMouse v3.60 protein database. The database was appended with commonly observed background proteins to prevent false assignment of peptides

derived from those proteins. Spectral count per protein were collected and reflect the number of matched peptides and the number of times those peptides were observed. Spectral counts were normalized to TnI (20S subunits) and actin (19S subunits) to allow for between group comparisons. Phosphopeptide enrichment and analysis using TiO2 was performed as described in Lu et al. (42).

Statistical analysis: Data are expressed as mean ± SEM unless otherwise indicated. Continuous variables were analyzed using 1-way ANOVA. 26S proteasome activity over a range of ATP concentrations was analyzed using 2-way repeated-measures ANOVA with Bonferroni adjustment for multiple comparisons. All statistical analysis was performed using Sigma Stat 3.0 or Microsoft Excel with $P<0.05$ indicating significant differences.

PART 1 RESULTS: The effects of sarcomere gene mutations on UPS function in hypertrophic cardiomyopathy (HCM)

Impairment of UPS activity in HCM and failing hearts compared to non-failing controls

Cardiac tissue was collected from hypertrophic cardiomyopathy (HCM), end-stage heart failure (F), and non-failing patients (NF). As expected, the HCM patients displayed remarkable LV wall thickness presenting a maximum wall thickness that was significantly increased in comparison to NF or F patients. In addition, HCM patients exhibited a significant increase in ejection fraction and systolic function, while F patients exhibited a significant decrease in ejection fraction and systolic function, in comparison to NF cardiac tissue (see ref 24 for

additional details on patient demographics). For the 29 HCM patients, 22 chose to undergo genetic testing and 14 of these 22 exhibited a pathogenic sarcomere gene mutations that has previously been reported to correlate with HCM. Within the HCM group, genetic testing identified mutations in *MYBPC3* (n=12), *TNNT2* (n=1), and *TPM1* (n=1).

Prior to my entry into the lab, chymotrypsin-like and caspase-like activity of the UPS was analyzed by Jaime Predmore in HCM, F, and NF tissue over a range of ATP concentrations using a synthetic fluorogenic peptides as substrates. Total chymotrypsin-like activity was significantly decreased in HCM and F samples in comparison to NF samples over the entire range of ATP ($p<0.001$, Figure 2A). Similarly, total caspase-like activity was markedly decreased in HCM and F compared to NF tissue at basal ATP and all exogenous ATP concentrations (Figure 2B). In addition, in order to more fully access the impairment of UPS the accumulation of polyubiquinated proteins in tissue homogenates was analyzed. Both HCM and F tissue showed an increase in the presence of polyubiquinated proteins compared to non-failing tissue, but only the increase in the F tissue was significant ($p<0.05$, Figure 2D and E) (24).

Proteasome subunit composition not altered in HCM and F compared to NF

There are several ways to explain the observed impairment of proteasomal activity in HCM and F tissue. One such explanation involves overall down regulation of proteasomal subunits. Therefore representative subunit expression was evaluated for the 20S, 19S, and 11S complexes. Upon investigation there was no significant difference in proteasomal subunit expression for α-7 (20S), Rpt-4, Rpt-1, Rpt-3, (19S ATPases), Rpt-10 (19S ubiquitin recognition site) and PA28α (11S) in HCM and F tissue compared to the NF control (Figure 3). These data suggest that the impairment of proteasome activity in HCM and F tissue cannot be explained by

a decrease in proteasomal subunit expression and led us to hypothesize that is was instead post-translational modifications to the proteasome. Recently published work in our lab suggests that oxidative modification plays an important role in regulating the activity of the UPS is F tissue (24), yet a mechanistic explanation for the observed decrease in UPS activity in HCM tissue remains in question.

Lower UPS activity in HCM samples with sarcomere mutations and decreased cMyBP-C expression in HCM samples with a variety of cMyBP-C mutations:

Over half of the cases of HCM are linked to mutations in myofilament genes. When comparing within the HCM group, chymotrypsin-like activity of HCM samples with pathogenic myofilament gene mutations showed markedly lowered activity than HCM samples without pathogenic mutations (Figure 4A). This finding is very intriguing given the results of a recent study, which shows that accelerated degradation of truncated mutants of the myofilament protein, cMyBP-C, impair the functional capabilities of the UPS in neonatal rat cardiac myocytes (25). cMyBP-C is a 140-kDa protein that belongs to the intracellular immunoglobin super family and, like other sarcomeric proteins is composed of repeating Ig and fibonectin type-3 domains. The cardiac isoform of MyBP-C differs from the skeletal form as the cardiac form possesses an extra Ig region (C0) and a phosphorylation domain (M) in between C1 and C2 (Figure 4B). Prior work has shown that cMyBP-C associates with the thin and thick filaments within the cardiac sarcomere and some evidence shows that cMyBP-C plays a role in myofibril assembly and organization (38).

We hypothesize that instability of mutant proteins within the sarcomere could lead to UPS dysfunction and have begun to study this relationship by investigating human heart tissue

from HCM patients who displayed one of the following cMyBP-C mutations: 6 premature truncations, 2 spice site variations, 2 inframe duplications or deletions, and 2 missense allele (Glu542Gln and Arg495Gln) (Figure 4B). In these samples, the absolute content of cMyBP-C protein was significantly reduced in hearts containing both truncated and full-length *MYBPC3* mutations (normalized densitometric ratio 61% ± 6) vs. human non-failing hearts (93% ± 8, $p<0.05$) or HCM hearts lacking sarcomere mutations (115% ± 12, $p<0.01$) (Figure 4C and D). However, no truncated mutant cMyBP-C proteins were detected by immunoblotting using an antibody that recognizes an N-terminal epitope of cMyBP-C. Interestingly, a single HCM patient who exhibited a cMyBP-C truncation (IVS20 2A>G) and progressed to end stage heart failure requiring a left ventricular assist device showed the lowest cMyBP-C expression of all tested samples. In contrast, total cMyBP-C expression was not reduced in other end stage failing heart samples of diverse etiologies (Figure 4E) suggesting that the observed decrease in cMyBP-C expression in IVS20 2A>G is not a consequence of the progression to heart failure.

mRNA expression levels within HCM samples with cMyBP-C mutations

The decrease in amount of total cMyBP-C expression in HCM samples with cMyBP-C mutations could be the result of decreased mRNA expression or transcript instability or accelerated protein degradation. I found that the total amount of mature cMyBP-C mRNA transcripts in the HCM tissue compared to non-failing donor control tissue was not significantly reduced (Figure 5). Interestingly, some individual samples did display a reduction in mRNA expression levels in comparison to the non-failing donor control, but the degree of reduction was far less than the overall reduction in cMyBP-C observed at the protein level suggesting that post translational protein processing may also contribute to the decrease in cMyBP-C expression.

In addition, I also sought to investigate the relative percentages of wild type and mutant mRNA transcripts within HCM samples with cMyBP-C mutations. Nonsense-mediate mRNA decay (NMD) specifically targets premature truncation(PTC)-bearing mRNAs for degradation when the PTC lies >50 to 55 nt upstream of the last exon-exon junction, which is the case with all the truncation mutations samples we have collected. Thereby, if NMD was degrading the truncation products at the mRNA level, this would explain why I failed to see the truncated mutant cMyBP-C at the protein level. To characterize the levels of different cMyBP-C mutant mRNAs, I created Taqman hydrolysis probes to recognize mutant mRNA or total cMyBP-C mRNA, and from these two assays, the percentage of mutant and wild type transcript could be calculated. I found that different sets of primer/probe did not amplify cMyBP-C cDNA with equal efficiencies and therefore I did not feel confident that I would be able to accurately quantify the relative amount of mutant and wild type mRNA transcripts in our HCM samples. Adjusting the primer/probe concentrations in the reactions did not significantly affect reaction efficiency, so I am currently working on adjusting the cDNA concentration to equalize efficiencies of each individual primer/probe set for each individual sample.

Quantification of the relative ratio of mutant and wild-type proteins in cMyBP-C R495Q missense mutations:

Another potential cellular mechanism that may contribute to the observed decrease in total cMyBP-C protein expression is degradation of the mutant proteins by the UPS. Previous studies in *in vitro* and animal model systems, along with limited data in human HCM hearts, have led to the widely accepted hypothesis that sarcomere gene mutations that result in premature truncations (>50% of *MyBPC3)* cause haploinsufficiency (35-37), while missense

mutations in full-length proteins (majority of non-*MyBPC3* mutations) exert their effects through a dominant-negative mechanism, maintaining sarcomere protein stoichiometry. In the latter case, the conventional belief is that the ratio of mutant to wild-type proteins is ~50:50 (38). In order to investigate this supposition using human tissue, and to determine if the decrease in total cMyBP-C expression is caused by a quantitative decrease in mutant proteins, absolute quantification of abundance (AQUA) analysis was performed to determine the relative ratios of mutant and wild-type proteins in a sample heterozygous for a full length cMyBP-C R495Q missense mutation.

As shown in Figure 4C this sample contained approximately half the amount of cMyBP-C expression compared to non-failing donor controls and according to the hypothesis within the literature, there should be an equal ratio of mutant and wild type cMyBP-C protein. To our surprise, AQUA analysis showed a 3:1 predominance of the missense protein to its wild-type counterpart (Figure 6). The increase presence of the mutant protein over the wild-type cMyBP-C suggests differential stability of the wild-type and mutant protein and/or a competitive advantage of the mutant protein over its wild-type counterpart for incorporation into the sarcomere. Additional studies are underway to investigate the ratio of mutant and wild-type proteins in patients that have other mutations in cMyBP-C, and to compare them to mutations in other sarcomere genes, including beta myosin heavy chain, troponin T, tropomyosin, and myosin light chain.

Effects of phosphorylation on cMyBP-C stability:

A unique feature of cMyBP-C is that it possesses three phosphorylation sites at residues Ser-273, Ser-282, and Ser-302 in its M domain. These sites, which are phosphorylated by PKA (all sites) and PKC (only Ser-273 and Ser-302) have been shown to play an important role in regulating overall cardiac function and in protecting cMyBP-C against degradation by the UPS

(39, 40). cMyBP-C phosphorylation within HCM samples was studied in samples with cMyBP-C mutations and non-failing donor controls to investigate if phosphorylation differences could explain overall decrease in total cMyBP-C expression and possibly provide insight into the observed decrease in UPS activity. There was no detectable change in the phosphorylation of Ser-302 standardized to total cMyBP-C in cMyBP-C mutants compared to non-failing donor controls and non-cMyBP-C mutant HCM samples (Figure 7). One interesting finding was that the IVS20 2A>G sample which exhibited the lowest level of overall cMyBP-C expression showed the highest level of Ser-302 of any of the samples tested. Species specificity of antibodies directed against phosphorylation at Ser-273 and Ser-282 has hampered studies of phosphorylation at these sites. I plan next to use phosphor-serine specific antibodies to study levels of total phosphorylation of cMyBP-C in HCM samples with cMyBP-C mutations compared to non-failing control tissue.

PART 1 DISCUSSION:

Our study provides direct evidence for the association between ubiquitin proteasome dysfunction and two human cardiac pathologies, hypertrophic cardiomyopathy and heart failure. Additionally, another important finding in this study is the significant decrease in UPS activity in HCM samples that possess pathogenic myofilament gene mutations compared to HCM samples that lack gene mutations. One earlier study described UPS impairment resulted from the accelerated degradation of cMyBP-C truncated mutants in an animal model (25), yet limited knowledge exists of the effects of myofilament mutations on the UPS activity in human tissue. Our study attempts to fill this gap in knowledge by measuring transcript and protein abundance

of mutant and wild type versions of cMyBP-C in an attempt to understand potential implications on the ubiquitin proteasome system in human tissue and in the pathogenesis of HCM.

Investigations of proteasomal activity within F and HCM hearts in comparison to NF tissues revealed several important findings. The most important finding relates to the marked inhibition of proteasomal activity of the UPS in F and HCM hearts compared to their non-failing counter parts. This difference in UPS activity is a novel finding that can potentially provide an important distinguishing factor between disease states and the non-failing control hearts. Similar to previous reports, polyubiquinated proteins were significantly increased in failing hearts compared to non-failing counterparts. Interestingly, in HCM hearts there was no observed increase in polyubiquinated proteins despite a similar reduction in UPS activity. This difference may be attributed to a difference in the duration of UPS dysfunction.

A previous explanation for decrease in UPS activity in an animal heart failure model included stoichiometric alterations to subunit expression within the 26S complex (7, 46). However, in our study we do not see any difference in subunit expression within the 20S proteolytic core, 19S regulatory cap, or the 11S activator. This observation points toward the importance of post-translational modification to explain alterations in UPS activity. A recent paper published by our lab shows that oxidative modifications may inhibit the UPS in F tissue, but the mechanistic explanation for alterations in UPS activity in HCM tissue has yet to be uncovered (24).

Prior studies on protein degradation in human cardiac disease have been confined to end-stage heart failure with limited investigation of hypertrophic cardiomyopathy (44). Over half the cases of hypertrophic cardiomyopathy are associated with mutations in sarcomere genes (45). We observed that proteasomal activity was significantly lower in patients with sarcomere gene

mutations compared to HCM patients without known genetic mutations. This finding parallels a previous animal study that showed truncation mutations in cardiac myosin binding protein C contribute to UPS dysfunction in neonatal rate myocytes (25). In addition, our results show that premature truncations, splice site variations, inframe duplications or deletions, and missense alleles (Glu542Gln and Arg495Gln) all result in an overall reduction of total cMyBP-C expression without a significant change in mRNA expression levels or phosphorylation at Ser-302 in patients with *MYBPC3* mutations.

An interesting finding of this study was the drastic reduction in cMyBP-C expression in a HCM patient (IVS20 2A>G) who progressed to end-stage systolic heart failure and showed the highest phosphorylation of Ser-302 per total cMyBP-C expression. Studies have shown that phosphorylation of the cardiac cMyBP-C motif, containing Ser-302, protect cMyBP-C proteins from degradation by the ubiquitin proteasome system (40). Thus, the marked reduction in cMyBP-C expression coupled with the significant increase in Ser-302 phosphorylation of IVS20 2A>G suggest cellular attempts to protect the remaining cMyBP-C from degradation of the UPS, possibly contributing to UPS impairment.

One of the most intriguing finding of this study was the 3:1 predominance of the cMyBP-C R495Q missence mutant protein over its wild-type counterpart. Previous studies *in vitro* and in animal models have hypothesized that mutations in myofilament genes that result in premature truncations cause haploinsufficiency (35-37), while missense mutations result in an approximate *50:50* ratio of mutant and wild-type producing a dominant negative effect (38). Yet, limited investigations into the expression of mutant and wild-type proteins have been conducted in human tissue. Our study, with the use of absolute quantification of abundance technology, provides the first analysis of the ratio of mutant and wild-type MyBP-C proteins in human

cardiac tissue. This finding is of significant interest as the patient heterozygous for the cMyBP-C R495Q missense mutation shows an approximate 50% decrease in overall cMyBP-C protein expression, yet this expression is not caused by complete degradation of the mutant protein. Instead the mutant protein is more highly expressed than its wild-type counterpart. We hypothesize that the decrease in protein expression of cMyBP-C coupled with the predominance of the mutant protein may result from differential stability of the mutant and wild-type protein possibly through aggregation of the mutant protein which interferes with the basal protein level of wild-type cMyBP-C. Immunolocalization and electron microscopic experiments are planned to investigate the possibility of protein aggregation and sarcomere disruption.

In conclusion, a marked decrease in UPS activity is observed in tissue from HCM and F patients compared to their NF counterparts. This decrease cannot be explained by a change in subunit expression and thereby suggests the importance of post-translational modifications and/or other cellular mechanisms in explaining UPS impairment. In addition, the presence of sarcomere gene mutations in HCM tissue contributes to a more profound inhibition in UPS activity then HCM tissue lacking sarcomere mutations and suggests that specific mutations in sarcomere proteins, such as cMyBP-C, may interfere with UPS function. In addition, our investigations on samples with cMyBP-C mutations show an overall decrease in protein expression without significant changes in mRNA expression levels or phosphorylation at Ser-302. Most importantly, quantification of the relative ratio of mutant and wild-type proteins suggests that the previous hypothesis developed in animal models of missense mutations in myofilament genes resulting in a dominant negative effect with an approximate 50:50 ratio of mutant to wild-type proteins may not hold completely true in human disease.

PART 2 RESULTS: Alterations in UPS activity in a mouse model of heart failure

Activation of the UPS in mice following left coronary artery ligation (LCA)

The effects of coronary artery occlusion on peptidase activity of the cardiac proteasome were evaluated utilizing an *in vivo* mouse model in which coronary occlusion was induced by ligating the left coronary artery producing a myocardial infarction (MI). For this model, the infarct size was approximately 40% and the survival rate was >70% in young female mice. Progression to heart failure was confirmed by echocardiography, which showed an increase in left ventricle size from 2 weeks to 6 months after MI. Prior to my entry into the lab, Jaime Predmore collected hearts 2, 4, and 8 weeks after MI and investigated chymotrypsin-like activity of the UPS within these samples across several different ATP concentrations. Chymotrypsin-like activity was not significantly different between Sham and infarcted mice prior to introduction of ATP (Figure 8). Upon the addition of ATP, peptidase activity in all samples rose and the ATP-dependent chymotrypsin-like activity was significantly higher in infarcted hearts 2, 4, and 8 weeks after myocardial infarction compared to Sham operated mice. As concentrations of ATP were increased, chymotrypsin-like activity in all samples was partially inhibited which has been also seen in previous studies (41), yet less inhibition occurred in infarcted hearts 2, 4, and 8 weeks after MI.

Proteasome subunit composition

In an attempt to explain this increase in activation of the UPS 2, 4, and 8 weeks following MI, the overall protein expression of representative subunits of the 11S (PA28α), 19S (Rpt4), and 20S (α-7) were investigated (Figure 9A and B). By immunoblotting methodology, there

were no significant differences between mice 2, 4, and 8 weeks after MI when compared to their Sham counterparts. Therefore, the inability of differences in proteasomal subunit content to explain the observed activation of the UPS points toward the possibility of a post-translation modification affecting UPS activity in our mouse model of heart failure.

Purification of the 19S and 20S UPS complexes

To gain further insights into potential post-translational modifications of the UPS following infarction, I needed to generate a highly purified preparation of the 19S and 20S proteasome. The development of a purification protocol that was both functional and feasible for our experimental purposes proved very complicated. Previous studies have purified the 19S and 20S complexes using extensive biochemical purification procedures that yield a highly enriched sample (8). For our purposes this procedure was not feasible as it required a significant number of mice (100 mice) to produce a single group for comparison. Thereby, I chose to use an immunoprecipatation procedure to purify the UPS complex. Initially, I attempted to use immunoprecipatation columns (Cell Signaling), however these columns did not allow for the co-immunoprecipatation of subunits from the 19S and 20S complexes from the mouse cardiac tissue. Therefore, I attempted to separately purify the 19S and 20S complexes, however again the immunoprecipatation columns failed to allow adequate purification of many subunits within each complex. I then decided to alter my protocol to optimize an immunoprecipatation procedure previously used in our lab and separately purify the 19S and 20S complexes using this procedure (see methods). After incorporation of phosphatase inhibitors to allow me to study phosphorylation of the UPS complexes following immunoprecipatation in this protocol I was

able to achieve a 33 and 30 fold enrichment of the 19S and 20S complexes respectively (Figure 10A).

Following the development of this immunoprecipation procedure 2-Dimensional gel electrophoresis (2DE) coupled with immunoblot detection was used to further verify the purification of proteasomal subunits. As shown in Figure 10B, subunits within the 20S (α-3) and 19S (Rpt-4) complexes were separated by 2DE and the identity of these subunits was confirmed with immunoblot detection. The molecule weight and isoelectric points of α-3 (29.47 kDa and 7.58 pI) and Rpt-4 (44.04 kDa and 7.25 pI) were remarkably consistent with their theoretical subunit masses and pI values (www.expasy.org). One potential problem with my immunoprecipation procedure coupled with 2DE analysis was that many additional proteins co-purified with the proteasomal subunits which may have resulted from proteins binding nonspecifically during the immunoprecipatation, proteins functionally associating with the UPS, or proteins being in the process of degradation by the UPS (Figure 10B). However, because of this procedure's ability to identify α-3 and Rpt-4 subunits with immunoblot detection, I chose to continue to use this protocol to study post-translational phosphorylation of the proteasomal subunits in an attempt to better understand the observed differences in UPS activity between Sham and infarcted mice.

Phosphorylation of the UPS in LCA mice model

Prior studies have shown the importance of Protein Kinase A (PKA)-dependent phosphorylation within the murine cardiac proteasome for both the activation of the proteasome and the overall subunit assembly (42, 43). Following the development of the immunoprecipatation procedure, 1-Dimensional gel electrophoresis, 2-Dimensional gel electrophoresis (2-DE), and immunoblotting were used to delineate the potential impact of PKA-

dependent phosphorylation on the 19S and 20S proteasomal complexes. The 20S complex did not react with an antibody designed to recognize PKA dependent phosphorylated substrates (data not shown), yet the 19S complex exhibited a prominent band at approximately 50 kDa. Comparison of the molecular weight of this PKA substrate reactive protein to the molecular weight of several 19S subunits suggests that Rpt-3 may be a phosphorylation target of PKA (Figure 11A). Yet, because of the relatively similar molecular weights of the Rpt-1, Rpt-3, and Rpn-5, 2-DE was used to create better subunit separation. 2-DE followed by immunoblotting studies suggested that the Rpt-3 subunit may be an endogenous target of PKA-dependent phosphorylation (Figure 11B). However analysis of the potential phosphorylated protein using MS/MS revealed that even though this protein aligned precisely with the Rpt-3 specific antibody, it was identified as mitochondrial Atp5b ATP synthase subunit beta. Further studies are underway to verify these findings, as the antibody recognition was so precise that it's possible that Atp5b ATP synthase and Rpt 3 could be co-localizing. Nevertheless, I felt that this technique was not going to sufficiently sensitive to detect phosphorylation of proteasome subunits and have therefore shifted toward using LC/MS/MS proteomic profiling.

This new approach allows for a comprehensive proteomic investigation of the UPS in Sham and infarcted mice. With this method, we were able to identify the relative expression of all subunits within the 20S complex (α1-α7, β1-β7, and PA200), the 11S complex (Pa28α, Pa28β, and Pa28γ), and the 19S complex (Rpt1-Rpt6, Rpn1-3, Rpn5-Rpn9, and Rpn11) except Rpn 4, 10, and 12 in hearts taken from both Sham and infarct mice. There were no significant differences in subunit expression in Sham vs. infarct mice confirming our previous immunoblotting results on selected subunits (Figure 12A-C). In addition, we also investigated differences in post-translational phosphorylation of the UPS subunits of Sham and infarct

through TiO2 enrichment (methods section). This study showed that the α-7 subunit was prominently phosphorylated in both Sham and infarct hearts, however there was no significant difference between the two groups (Figure 12D). This experiment is currently being repeated with additional starting material to both confirm the previous result and attempt to increase the sensitivity to detect other phosphorylated subunits of the UPS.

PART 2 DISCUSSION:

In this study, we show that the development of cardiomyopathy in a myocardial infarction mouse model is associated with an increase in activity of the ubiquitin proteasome system. This finding is consistent with an earlier study that described hyperactivation of the murine cardiac UPS following aortic constriction (28), but challenges data presented in a similar model that suggested an overall decrease in UPS activity contributed to progression to heart failure (27). Another important finding in the present study is that the observed alteration in proteasomal activity cannot be explained by differences in the expression of proteasomal subunits or the phosphorylation of the α-7 subunit.

Our investigation of proteasomal activity revealed several unique findings. First, there was a marked increase in chymotrypsin-like activity in LCA mice 2, 4, and 8 weeks after MI. This increase in activity paralleled the remodeling of the heart (49) suggesting that consistent over activation of the UPS correlates with the progression of a pathogenic phenotype. Second, our studies also revealed that inhibition of proteasome activity with increasing ATP concentrations was attenuated in infarcted mice in contrast to Sham operated mice. Although a similar response of UPS activity to increases in ATP concentrations has been previously observed in rat hearts (41), the reason for proteasomal inhibition with increasing concentrations

of ATP is currently unknown, but is likely to biologically important given that ATP-dependent proteasome activation is altered in pathologic states in both human and mouse cardiomyopathies.

Although several previous studies have found alterations in subunit expression accompanying variations in UPS activity (46, 47), my comprehensive, proteomics-based investigation of the expression of proteasomal subunits did not reveal any differences between groups. The fact that we did not observe differences in proteasomal subunit content between Sham and infarcted mice, suggests that post-translational modifications may play a role in regulating activity of the ubiquitin proteasome system under pathologic conditions.

To analyze phosphorylation of the proteasome we pursued a proteomic approach using an immunoprecipatation enrichment coupled with 2DE and immunoblot detection. Although this method successfully enriched for the cardiac proteasome and was able to separate and identify several proteasomal subunits, it was insufficiently sensitive to study phosphorylation within the proteasome due to co-purification of a large number of non-proteasome proteins. Thereby we shifted our approach toward LC/MS/MS proteomic profiling to obtain a comprehensive investigation of the UPS and potential phosphorylation differences. This method proved extremely advantageous as it allowed me to identify all proteasomal subunits within the 11S, 20S, and 19S complexes (except Rpn 4, 10, and 12 within the 19S) further confirming that there was no difference in subunit expression between the Sham and infarcted hearts. In addition, this procedure also showed that there was no difference in the phosphorylation of the α-7 subunit in Sham and infarcted hearts. The α-7 subunit is the most heavily phosphorylated subunit of the 20S proteasome and that its phosphorylation aids in the stabilization of the 26S complex (43). The inability to detect differences in α-7 phosphorylation between control and infarcted hearts suggests an alternate mechanism for the observed differences in proteolytic activity.

In order to determine if the observed increase in proteasome activity reflects a higher functioning proteasome, or if the increase in activity is a compensation for inadequate function of the UPS to process and degrade substrates, we are collaborating with Dr. XueJun Wang's group (University of South Dakota) on mice engineered with a in vivo reporter for UPS function (50).

In conclusion, a significant increase in the activity of the ubiquitin proteasome system was observed following MI. This increase in activity cannot be explained through alterations in the expression of the UPS subunits or alterations in the stability of the 26S proteolytic complex resulting from phosphorylation of the α-7 subunit. Future work will be necessary to uncover the mechanistic explanation for the observed increase in UPS activity.

Acknowledgements

I would like to thank Jaime Predmore for her work on the ubiquitin proteasome activity assay and David Allen and Richard Jones from NextGen Sciences Inc. for their help with the AQUA analysis and the LC/MS/MS analysis. In addition, I would like to greatly thank my research P.I., Dr. Sharlene Day, for her support and guidance throughout my research investigations.

References

1. Goldberg AL. Protein degradation and protection against misfolded or damaged proteins. *Nature* 2003; 426: 895-899.

2. Sudakin V, Ganoth D, Dahan A, Heller H, Hershko J, Luca FC, Ruderman JV, Hershko A. The cyclosome, a large complex containing cyclin-selective ubiquitin ligase activity, targets cyclins for destruction at the end of mitosis. *Mol. Biol. Cell* 1995; 6: 185-197.

3. Aberle H, Bauer A, Stappert J, Kispert A, Kemler R. β-catenin is a target for the ubiquitin–proteasome pathway. *EMBO.* 1997; 16:3797-3804

4. Maki CG, Huibregtse JM, Howley PM. In vivo ubiquitination and proteasome-mediated degradation of p53(1). *Cancer Res.* 1996; 56 2649-2654.
5. Hershko A. The ubiquitin system. *Annu. Rev. Biochem* 1998; 67: 425-479.
6. Groll M, Bajorek M, Kohler A, Moroder L, et al. A gated channel into the proteasome core particle. *Nat Struct Biol* 7: 1062-1067, 2000.
7. Moore DJ, Dawson VL, and Dawson TM. Role for the ubiquitin-proteasome system in Parkinson's disease and other neurodegenerative brain amyloidoses. *Neuromolecular Med* 4: 95-108, 2003.
8. Gomes AV, Zong C, Edmondson RD, et al. The murine cardiac 26S proteasome: an organelle awaiting exploration. *Ann N Y Acad Sci* 1047: 197-207, 2005.
9. Satoh K, Sasajima H, Nyoumura KI, et al. Assembly of the 26S proteasome is regulated by phosphorylation of the p45/Rpt6 ATPase subunit. *Biochemisty* 40: 314-319, 2001.
10. Baumeister W, Walz J, Zuhl F, and Seemuller E. The proteaseom: paragidm of a self-compartmentalizing protease. *Cell*. 1998; 92: 367-380.
11. DeMartino GN. Purification of PA700, the 19S regulatory complex of the 26S proteasome. *Methods Enzymol*. 2005; 398: 295-306.
12. Glickman MH, Ciechanover A. The ubiquitin-proteasome proteolytic pathway: destruction for the sake of construction. *Physiol Rev*. 2002; 82(2): 373-428.
13. Zhang F, Hu Y, Huang P, Toleman CA, Paterson AJ, Kudlow JE. Proteasome function is regulated by cyclic AMP-dependent protein kinase through phosphorylation of Rpt6. *J Biol Chem.* 2007;282(31):22460-22471.
14. Zong C, Gomes AV, Drews O, Li X, Young GW, Berhane B, Qiao X, French SW, Bardag-Gorce F, Ping P. Regulation of murine cardiac 20S proteasomes: role of associating partners. *Circ Res.* 2006;99:372-380.
15. Mason GG, Hendil KB, Rivett AJ. Phosphorylation of proteasomes in mammalian cells. Identification of two phosphorylated subunits and the effect of phosphorylation on activity. *Eur J Biochem.* 1996; 238:453-462.
16. Wang J, Maldonado MA. The ubiquitin-proteasome system and its role in inflammatory and autoimmune diseases. *Cell Mol Immunol.* 2006;3:255-261.
17. Andersson M, Sjostrand J, and Karlsson J. Differential Inhibition of Three Peptidase Activities of the Proteasome in Human Lens Epithelium by Heat and Oxidation. *Exp. Eye Res.* 1998; 67: 425-479.
18. Attaix D, Ventadour S, Codran A, Bechet D, Taillandier D, Combaret L. The ubiquitin-proteasome system and skeletal muscle wasting. *Essays Biochem.* 2005;41:173-186.
19. Bedford L, Hay D, Devoy A, Paine S, Powe DG, Seth R, Gray T, Topham I, Fone K, Rezvani N, Mee M, Soane T, Layfield R, Sheppard PW, Ebendal T, Usoskin D, Lowe J, Mayer RJ. Depletion of 26S proteasomes in mouse brain neurons causes neurodegeneration and Lewy-like inclusions resembling human pale bodies. *J Neurosci.* 2008;28:8189-8198.
20. Bennett EJ, Bence NF, Jayakumar R, Kopito RR. Global impairment of the ubiquitin-proteasome system by nuclear or cytoplasmic protein aggregates precedes inclusion body formation. *Mol Cell.* 2005;17:351-365.
21. Chen Q, Liu JB, Horak KM, Zheng H, Kumarapeli AR, Li J, Li F, Gerdes AM, Wawrousek EF, Wang X. Intrasarcoplasmic amyloidosis impairs proteolytic function of proteasomes in cardiomyocytes by compromising substrate uptake. *Circ Res.* 2005;97:1018-1026.

22. Bulteau AL, Lundberg KC, Humphries KM, Sadek HA, Szweda PA, Friguet B, Szweda LI. Oxidative modification and inactivation of the proteasome during coronary occlusion/reperfusion. *J Biol Chem.* 2001;276:30057-30063.
23. Powell SR, Wang P, Katzeff H, Shringarpure R, Teoh C, Khaliulin I, Das DK, Davies KJ, Schwalb H. Oxidized and ubiquitinated proteins may predict recovery of postischemic cardiac function: essential role of the proteasome. *Antioxid Redox Signal.* 2005;7:538-546.
24. Predmore J, Wang P, Davis F, Bartolone S, Westfall M, Dyke D, Pagani F, Powell S, Day S. Ubiquitin Proteasome Dysfunction in Human Hypertrophic and Dilated Cardiomyopathies. *Circ.* 2010: 121;997-1004.
25. Sarikas A, Carrier L, Schenke C, Doll D, Flavigny J, Lindenberg KS, Eschenhagen T, Zolk O. Impairment of the ubiquitin-proteasome system by truncated cardiac myosin binding protein C mutants. *Cardiovasc Res.* 2005;66:33-44.
26. Herrmann J, Lerman LO, Lerman A. Ubiquitin and ubiquitin-like proteins in protein regulation. *Circ Res.* 2007;100(9):1276-1291.
27. Tsukamoto O, Minamino T, Okada K, Shintani Y, Takashima S, Kato H, Liao Y, Okazaki H, Asai M, Hirata A, Fujita M, Asano Y, Yamazaki S, Asanuma H, Hori M, Kitakaze M. Depression of proteasome activities during the progression of cardiac dysfunction in pressure-overloaded heart of mice. *Biochemical and biophysical research communications.* 2006;340:1125-1133.
28. Depre C, Wang Q, Yan L, Hedhli N, Peter P, Chen L, Hong C, Hittinger L, Ghaleb B, Sadoshima J, Vatner DE, Vatner SF, Madura K. Activation of the cardiac proteasome during pressure overload promotes ventricular hypertrophy. *Circulation.* 2006;114:1821-1828.
29. Stansfield WE, Tang RH, Moss NC, Baldwin AS, Willis MS, Selzman CH. Proteasome inhibition promotes regression of left ventricular hypertrophy. *Am J Physiol Heart Circ Physiol.* 2008;294:H645-650.
30. Kostin S, Pool L, Elsasser A, Hein S, Drexler HC, Arnon E, Hayakawa Y, Zimmerman R, Bauer E, Klovekorn WP, and Schaper J. Myocytes die by multiple mechanisms in failing human hearts. *Circ Res.* 2003; 92: 715-724.
31. Weeker J, Morrison K, Mullen A, Wait R, Barton P, and Dunn J. Hyperubiquitination of proteins in dilated cardiomyopathy. *Proteomics.* 2003; 3: 208-216.
32. Davies KJ. Degradation of oxidized proteins by the 20S proteasome. *Biochimie.* 2001;83(3-4):301-310.
33. Shringarpure R, Grune T, Mehlhase J, Davies KJ. Ubiquitin conjugation is not required for the degradation of oxidized proteins by proteasome. *J Biol Chem.* 2003;278(1):311-318.
34. Bulteau AL, Lundberg KC, Humphries KM, Sadek HA, Szweda PA, Friguet B, Szweda LI. Oxidative modification and inactivation of the proteasome during coronary occlusion/reperfusion. *J Biol Chem.* 2001;276(32):30057-30063.
35. Van Dijk S, Dooijes D, Remedios C, Michels M, Lamers, Winegrad S, Carrier L, van der Velden J. Cardiac Myosin-Binding Protein C Mutations and Hypertrophic Cardiomyopathy: Haploinsufficiency, Deranged Phosphorylation, and Cardiomyocyte Dysfunction. *Circ.* 2009; 119:1473-81.
36. Rottbauer W, Gautel M, Zehelein J, Labeit S, Franz WM, Fischer C, Vollrath B, Mall G, Dietz R, Kübler W, Katus HA. Novel splice donor site mutation in the cardiac myosin-

binding protein-C gene in familial hypertrophic cardiomyopathy: characterization of cardiac transcript and protein. *J Clin Invest*. 1997;100:475– 482.

37. Moolman JA, Reith S, Uhl K, Bailey S, Gautel M, Jeschke B, Fischer C, Ochs J, McKenna WJ, Klues H, Vosberg HP. A newly created splice donor site in exon 25 of the MyBP-C gene is responsible for inherited hypertrophic cardiomyopathy with incomplete disease penetrance. *Circ*. 2000;101:1396 – 402.

38. James J, Zhang Y, Osinska H, Sanbe A, Klevitsky R, Hewett T, Robbins J. Transgenic Modeling of a Cardiac Troponin I Mutation Linked to Familial Hypertrophic Cardiomyopathy. *Circ Res.* 2000;87; 805-811.

39. Gautel M, Zuffardi O, Freiburg A, Labeit S. Phosphorylation switches specific for cardiac isoform of myosin binding protein C: a modulator of cardiac contraction? *EMBO J* 1995; 14: 1952-60.

40. Sadayappan S, Osinska H, Klevitsky, Lorenz JN, Sargent M, Molkentin JD, et al. Cardiac myosin binding protein-C phosphorylation is cardioprotective. *Proc Natl Acd Sci USA* 2006;103:16918-23.

41. Powell SR, Davies KJ, Divald A. Optimal determination of heart tissue 26S-proteasome activity requires maximal stimulating ATP concentrations. *J Mol Cell Cardiol.* 2007;42(1):265-269.

42. Lu H, Zong C, Wang Y, Young GW, Deng N, Souda P, Li X, Whitelegge J, Drews O, Yang PY, Ping P. Revealing the dynamics of 20S proteasome phosphoproteome: A combined CID and ETD approach. *Mol Cell Proteomics.* 2008.

43. Bose S, Stratford FL, Broadfoot KI, Mason GG, Rivett AJ. Phosphorylation of 20S proteasome alpha subunit C8 (alpha7) stabilizes the 26S proteasome and plays a role in the regulation of proteasome complexes by gamma-interferon. *Biochem J.* 2004;378(Pt 1):177-184.

44. Sanbe A, Osinska H, Saffitz JE, Glabe CG, Kayed R, Maloyan A, Robbins J. Desmin-related cardiomyopathy in transgenic mice: a cardiac amyloidosis. *Proc Natl Acad Sci U S A.* 2004;101(27):10132-10136.

45. Van Driest SL, Ommen SR, Tajik AJ, Gersh BJ, Ackerman MJ. Sarcomeric genotyping in hypertrophic cardiomyopathy. *Mayo Clin.Proc.* 2005;80(4):463-469.

46. Hall JL, Birks EJ, Grindle S, Cullen ME, Barton PJ, Rider JE, Lee S, Harwalker S, Mariash A, Adhikari N, Charles NJ, Felkin LE, Polster S, George RS, Miller LW, Yacoub MH. Molecular signature of recovery following combination left ventricular assist device (LVAD) support and pharmacologic therapy. *Eur Heart J.* 2007;28(5):613-627.

47. Gomes AV, Zong C, Edmondson RD, Li X, Stefani E, Zhang J, Jones RC, Thyparambil S, Wang GW, Qiao X, Bardag-Gorce F, Ping P. Mapping the murine cardiac 26S proteasome complexes. *Circ Res.* 2006;99(4):362-371.

48. Wolff MR, Buck SH, Stoker SW, Greaser ML, Mentzer RM. Myofibrillar calcium sensitivity of isometric tension is increased in human dialted cardiomyopathies. *J. Clin. Invest.* 1996; 98(1):167-76.

49. Day SM, Westfall MV, Fomicheva EV, Hoyer K, Yasuda S, La Cross NC, D'Alecy LG, Ingwall JS, Metzger JM. Histidine button engineered into cardiac troponin I protects the ischemic and failing heart. *Nat Med.* 2006 Feb;12(2):181-9.

50. Depre C, Powell SR, Wang X. The role of the ubiquitin-proteasome pathway in cardiovascular disease. *Cardiovasc Res*. 2010 Jan 15;85(2):251-2.

Figure 1

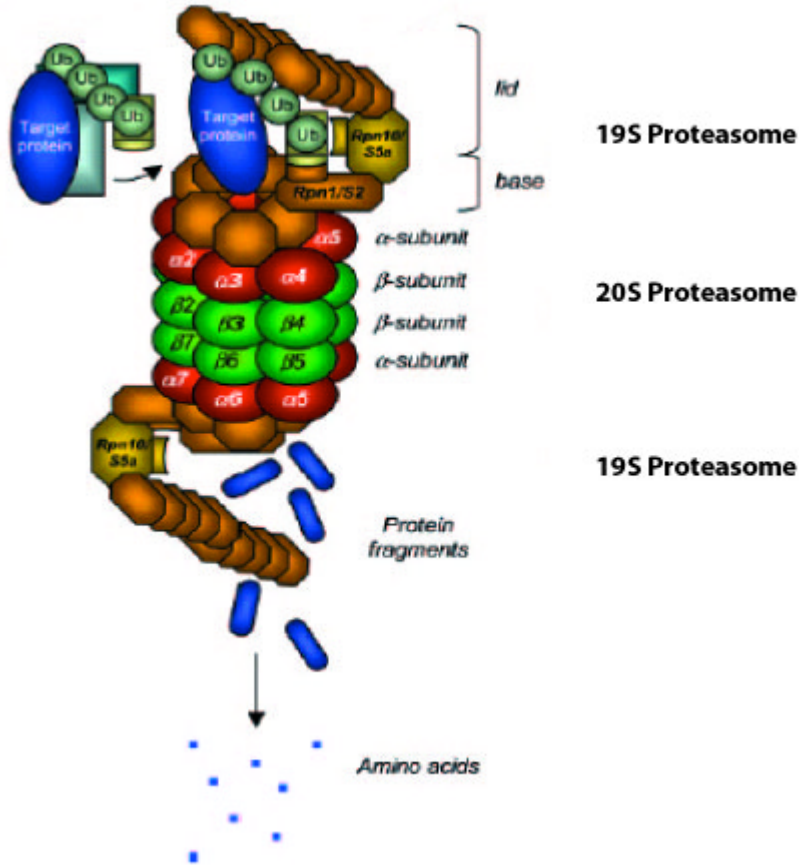

Figure 1. Ubiquitin Proteasome System

Configuration of the 26S proteasome and its accompanying subunits that coordinate degradation of polyubiquinated proteins. Adapted from Herrmann et al. (26).

Figure 2

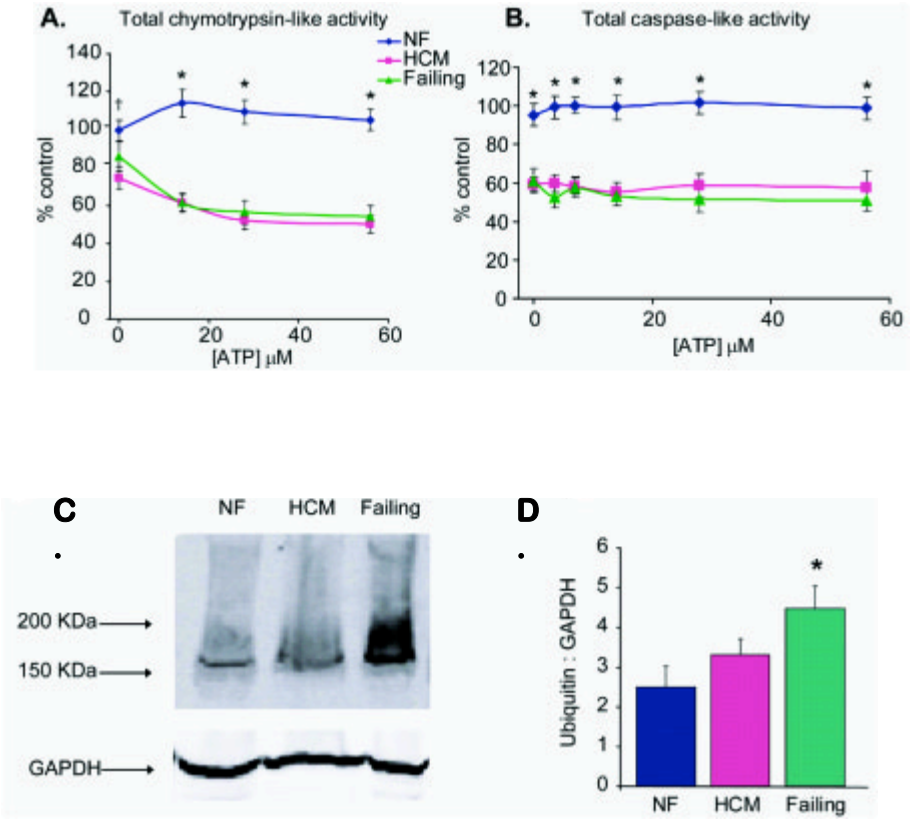

Figure 2. UPS activity and accumulation of ubiquinated proteins in NF, HCM, and F tissue samples.

A. Heart tissue homogenates (60 μg total cytosolic protein) were assayed for proteasome peptidase activity in the presence of increasing concentrations of ATP. Total chymotrypsin-like activity represents the difference in fluorescence in the presence and absence of the specific inhibitor, lactacystin (18 μmol/L). †P<0.05 for NF (n=6) vs. HCM (n=17). *P<0.01 for NF vs. HCM and NF vs. Failing (n=14). **B.** Total caspase-like activity represents the difference in fluorescence in the presence and absence of the specific inhibitor, ZPNAC (10 μmol/L). *P<0.01 for NF (n=5) vs. HCM (n=8) and NF vs. Failing (n=8). Proteasomal activity assays were provided by Jaime Predmore. **C.** Representative immunoblot of human total protein homogenates (50 μg) probed with an antibody against polyubiquinated proteins. **D.** Densitometric analysis for polyubiquinated proteins (>100KDa), standardized to GAPDH as a protein loading control. N=5 (NF), 11 (HCM), 10 (failing). *P<0.05 for NF vs. failing.

Figure 3

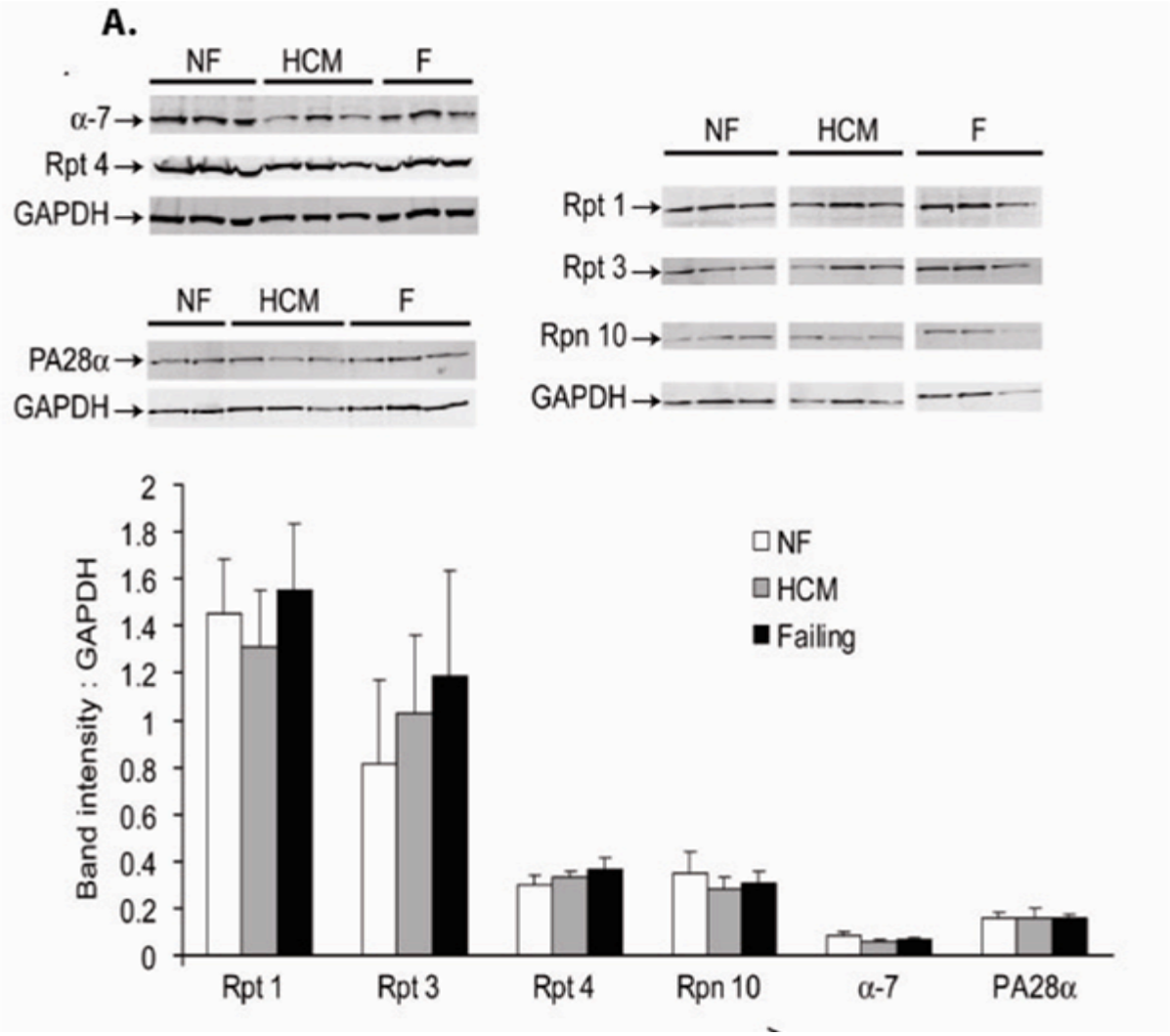

Figure 3. Proteasome subunit protein quantification in human tissue homogenates from NF, HCM, and F samples. Representative immunoblots for the core 20S (α-7), regulatory 19S cap (Rpt-1, Rpt-3, Rpt-4, and Rpn-10) and 11S activator (PA28α). Densiometric analysis of subunit expression standardized to GAPDH shows no significant difference in expression between HCM and F in comparison to NF control. N=5-12 per group.

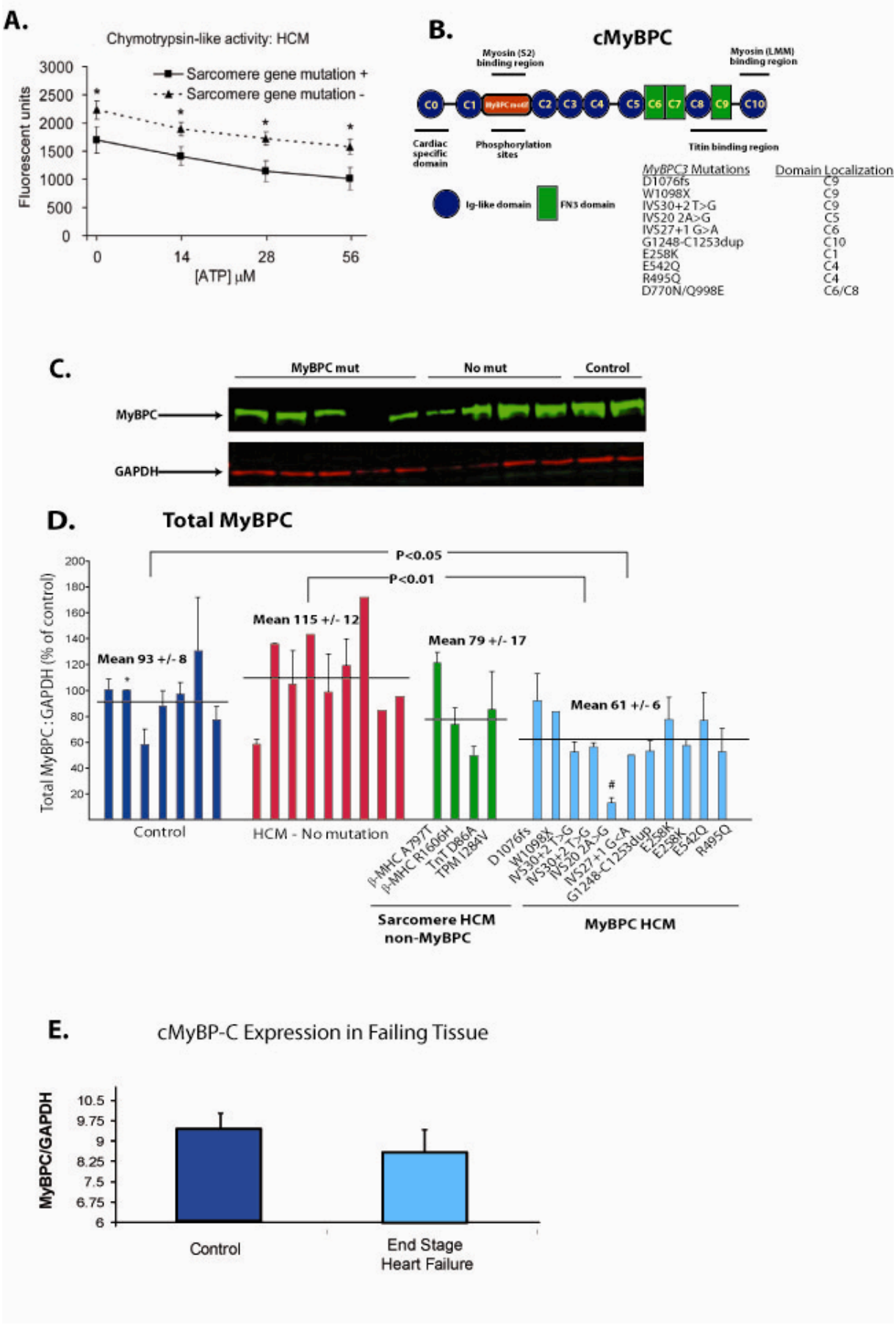
A.
Chymotrypsin-like activity: HCM
Sarcomere gene mutation +
Sarcomere gene mutation -
Fluorescent units
3000
2500
2000
1500
1000
500
0
0
14
28
56
[ATP] μM
B.
cMyBPC
Myosin (S2) binding region
Myosin (LMM) binding region
C0
C1
MyBPC motif
C2
C3
C4
C5
C6
C7
C8
C9
C10
Cardiac specific domain
Phosphorylation sites
Titin binding region
Ig-like domain
FN3 domain
MyBPC3 Mutations
Domain Localization
D1076fs C9
W1098X C9
IVS30+2 T>G C9
IVS20 2A>G C5
IVS27+1 G>A C6
G1248-C1253dup C10
E258K C1
E542Q C4
R495Q C4
D770N/Q998E C6/C8
C.
MyBPC mut
No mut
Control
MyBPC
GAPDH
D.
Total MyBPC
P<0.05
P<0.01
Total MyBPC : GAPDH (% of control)
200
180
160
140
120
100
80
60
40
20
Mean 93 +/- 8
Mean 115 +/- 12
Mean 79 +/- 17
Mean 61 +/- 6
Control
HCM - No mutation
β-MHC A797T
β-MHC R1606H
TnT D86A
TPM 1284V
D1076fs
W1098X
IVS30+2 T>G
IVS30+2 T>G
IVS20 2A>G
IVS27+1 G<A
G1248-C1253dup
E258K
E258K
E542Q
R495Q
Sarcomere HCM non-MyBPC
MyBPC HCM
E.
cMyBP-C Expression in Failing Tissue
MyBPC/GAPDH
10.5
9.75
9
8.25
7.5
6.75
6
Control
End Stage Heart Failure

Figure 4. Effects of Sarcomere Mutant Expression, specifically cMyBP-C mutations, on the UPS

A. Comparison of chymotrypsin-like activity in samples from HCM patients with or without sarcomere gene mutations. *P<0.05 for mutation positive (n=6) vs. mutation negative (n=7). **C.** Representative immunoblot comparing expression of total cMyBP-C in heart tissue from HCM patients in whom no sarcomere mutations were identified by clinical genetic testing, patients with non-*MyBPC3* sarcomere mutations, patients with *MyBPC3* mutations, and non-failing donors as controls. As previously reported, no truncated mutant cMyBP-C mutant proteins were detected. **D.** Densitometric analysis of cMyBP-C expression, relative to GAPDH as a loading control and expressed as a percentage of a single control sample (*). There was a significant decrease in total MyBP-C expression in HCM tissue samples with *MyBPC3* mutations compared to HCM samples that did not have *MyBPC3* mutations (P<0.01) and control tissue (P<0.05). # IVS20 2A>G was from the apex of a patient who underwent left ventricular assist device implantation for end stage systolic heart failure. **E.** Densitometric analysis of cMyBP-C expression, relative to GAPDH as a loading control, in non-failing donors as controls vs. patients with end-stage heart failure. cMyBP-C levels were not significantly reduced (p=0.44) in samples obtained from patients with end stage heart failure of various etiologies.

Figure 5

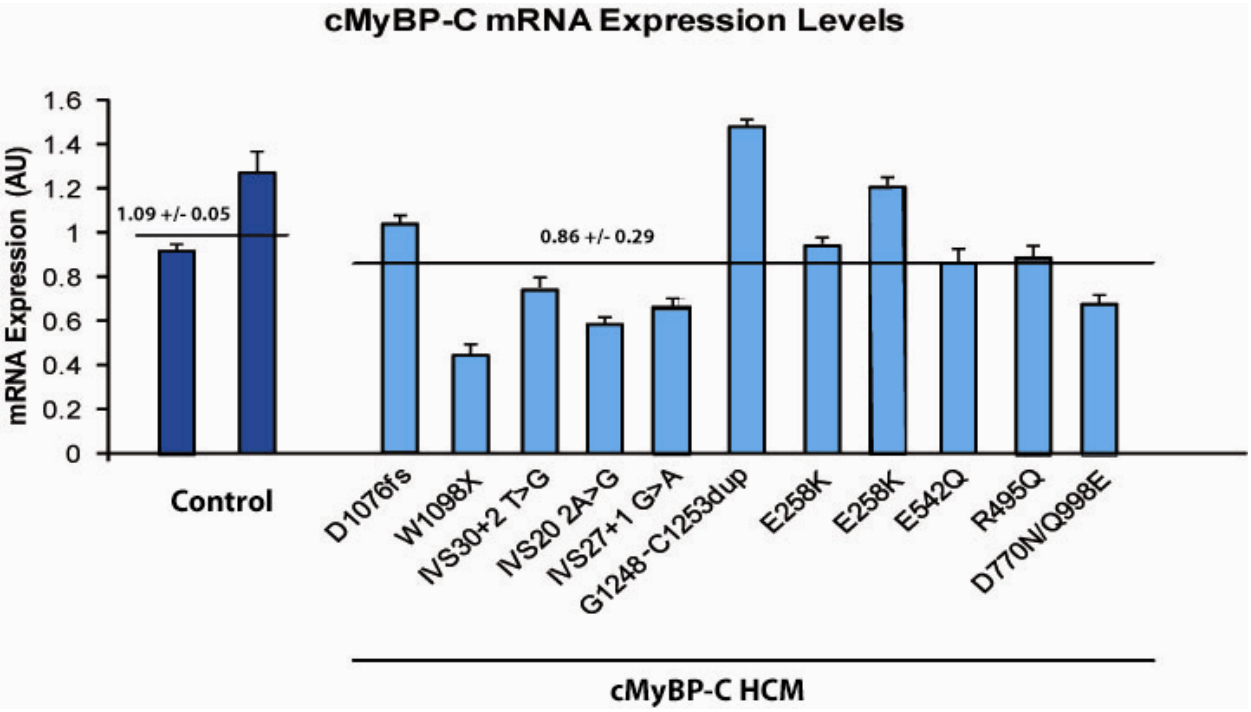

Figure 5. Quantification of mRNA transcripts in HCM tissue with cMyBP-C mutations and non-failing donor control. Hydrolysis probe analysis of mRNA expression relative to β-actin as an endogenous referent in non-failing donor control samples and tissue HCM containing cMyBP-C mutations gene. The results are expressed as a percentage of the average expression of the two control samples with intra-assay standard error within each sample shown as error bars. There was no significant decrease ($p=0.317$) in cMyBP-C mRNA expression from HCM samples that contained *MYBPC3* mutations compared to the non-failing controls.

Figure 6

cMyBPC

cMyBPC R495Q						Wild-type cMyBPC				
	Peak area		Ratio			Peak area		Ratio		
Sample	Endogenous Peptide	AQUA Peptide	(Endogenous/ AQUA)	Av. Ratio	Stdev.	Endogenous Peptide	AQUA Peptide	(Endogenous/ AQUA)	Av. Ratio	Stdev.
R495Q	4408310	247361	17.8	15.3	3.5	1115242	189796	5.9	5.3	0.8
	5430943	422033	12.9			1311945	279324	4.7		

Sample	Peptide	Calculated fmol	Percentage
Q495	Mutant	153.4	74.4%
R495	Wild type	52.9	25.6%

Figure 6. Absolute quantification of abundance (AQUA) methodology used to compute the stoichiometric ratios of full length mutant proteins relative to wild-type for cMyBP-C R495Q. Wild-type and mutant AQUA peptides were synthesized using heavy K isotopes as described in the methods section. Endogenous cMyBP-C proteins from human HCM hearts were gel extracted and digested with Lys-C. Peptide mixtures were spiked with 2µL of 10 fmol/µL solution of the corresponding AQUA peptides and analyzed in duplicate by LC/SRM. Peak areas were calculated using the Thermo Qual Browser Software. Peak areas for endogenous peptides were divided by peak areas of AQUA peptides to yield a relative mole ratio of endogenous mutant: wild-type peptides. Results show a 3:1 predominance of the mutant peptide over its wild-type counterpart.

Figure 7

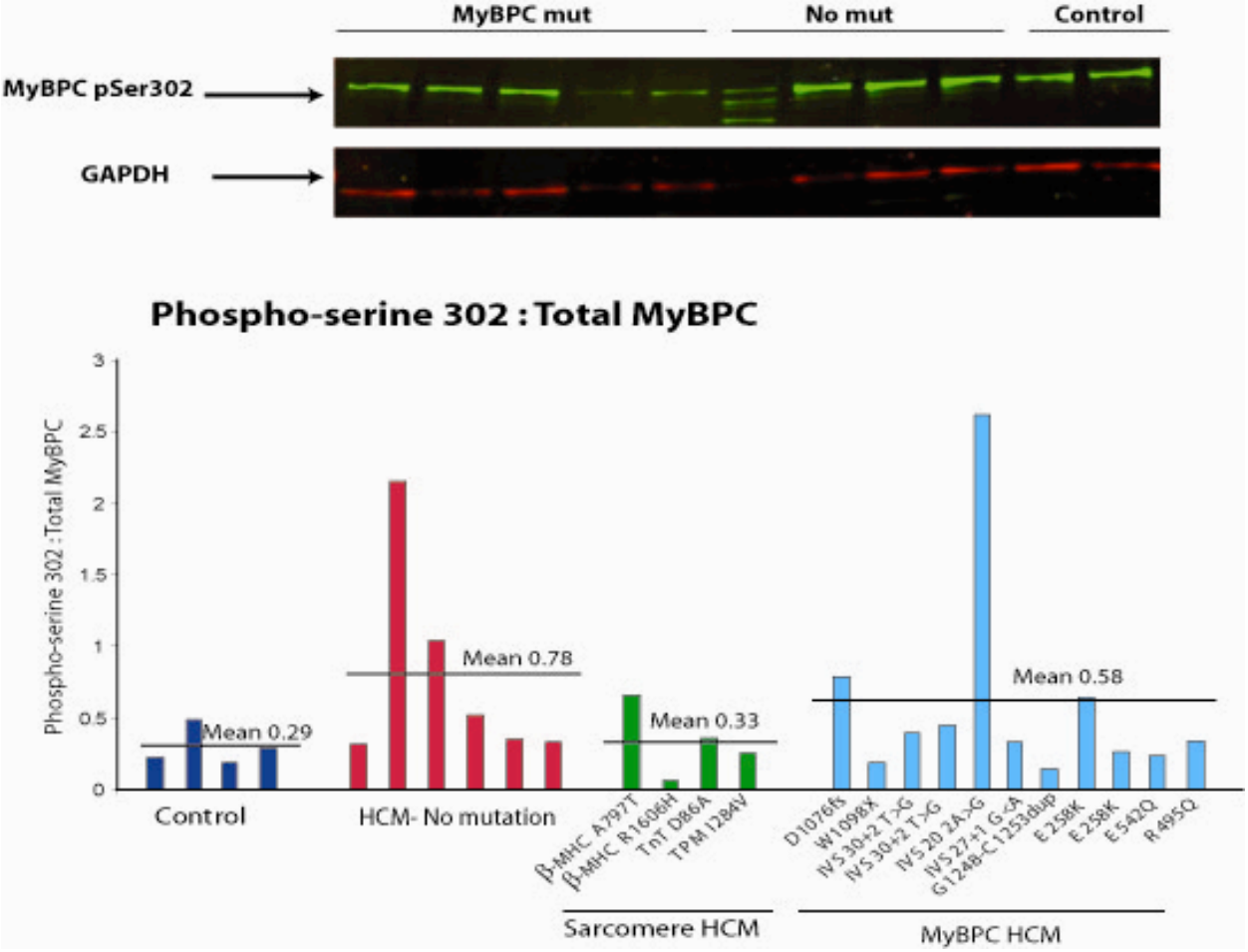

Figure 7. Phosphorylation of cMyBP-C at Ser-302 shows no significant difference. Representative immunoblot of phosphorylated cMyBPC at Ser-302 in HCM tissue samples containing *MYBPC3* mutations, HCM tissue samples lacking sarcomere mutations, HCM tissue with non-*MYBPC3* sarcomere mutations and control tissue. Densitometric analysis of phospho-cMyBP-C expression was calculated relative to GAPDH as a loading control and expressed as a ratio of total cMyBP-C. There was no significant difference in pSer302 detection among the groups. Antibodies against phospho-serine 273 and phospho-serine 282 of cMyBP-C were not reactive with human tissue.

Figure 8

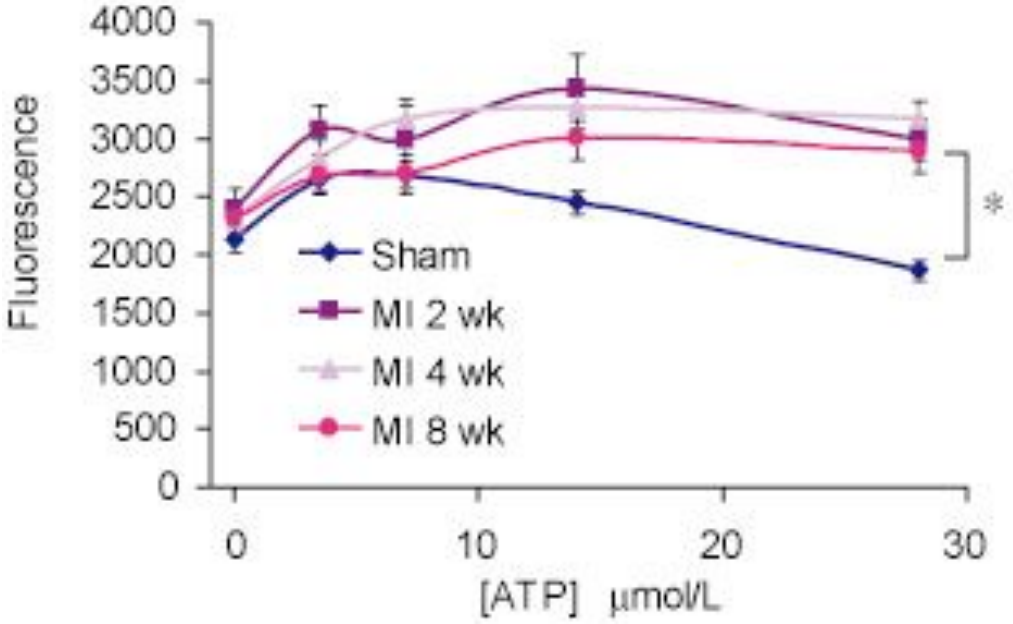

Figure 8. Chymotrypsin-like activity in sham vs. infarcted (MI) mouse hearts. Chymotrypsin-like activity is calculated as the difference in fluorescence in the presence and absence of lactacystin (18 µmol/L), a specific inhibitor of chymotrypsin-like activity. Sham (n=25, pooled) and MI (n=3 per group). *Overall $P<0.05$ for the difference between sham and MI at 2 and 4 weeks. This work was provided by Jaime Predmore.

Figure 9

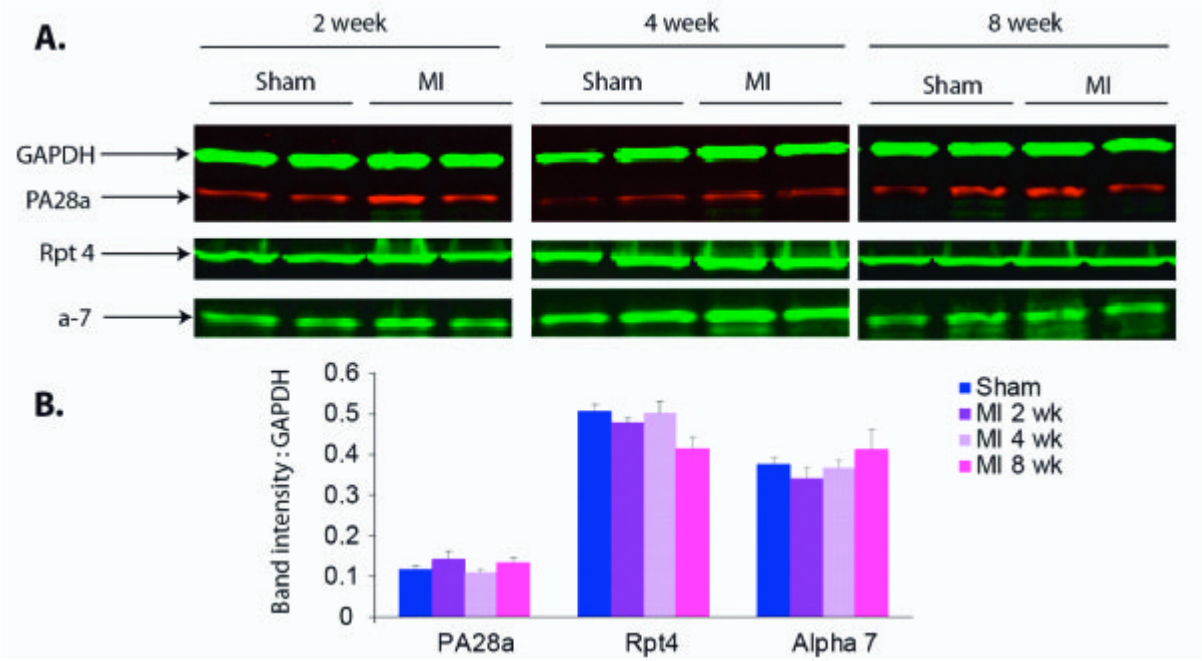

Figure 9. Proteasome subunit protein quantification in mouse whole heart homogenates. A. Representative immunoblots probed for proteasome subunits from the 20S core (α-7), 19S regulatory cap (Rpt 4), and 11S activator (PA28α) (top). **B.** Densitometric analysis of subunit protein content relative to GAPDH as a protein loading control (bottom). There were no significant differences in protein expression of any of the subunits among groups. N=5-12 per group.

Figure 10

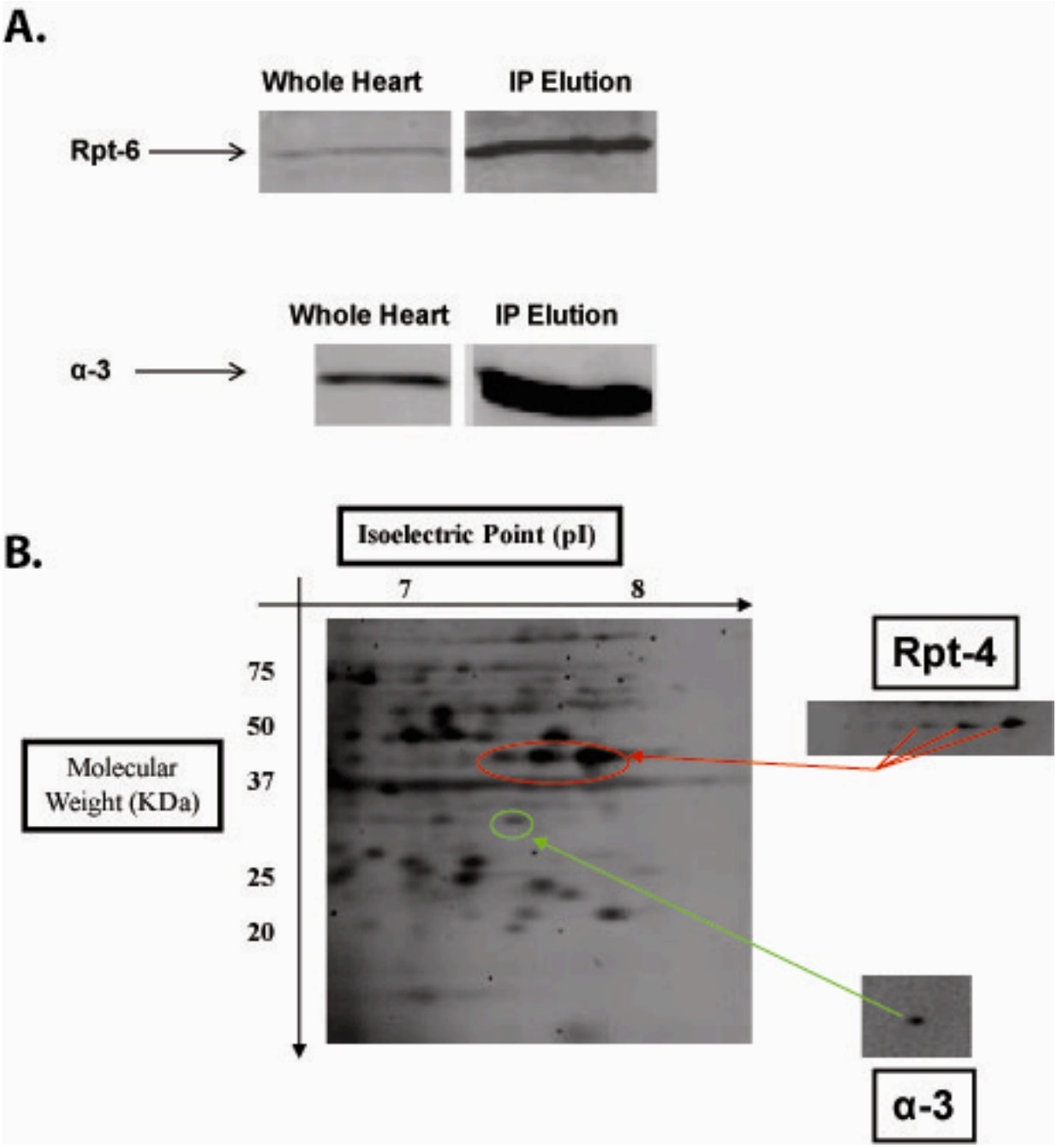

Figure 10. Immunoprecipatation of murine cardiac UPS and analysis via 2-Dimensional gel electrophoresis. A. Representative immunoblots of 15 µg of whole-heart homogenate or elution product from immunoprecipatation protocol probed with antibodies against Rpt-6 for the 19S complex and α-3 for the 20S complex. **B.** 2DE of purified 19S and 20S complex stained with SYPRO RUBY stain for total protein. The panels on the right correspond to representative immunoblots of 2-Dimnesional separation of the UPS probed with antibodies designed to

recognize Rpt-4 or α-3. Images of these blots were overlaid onto the protein stained gel to locate the relative position of the proteins.

Figure 11

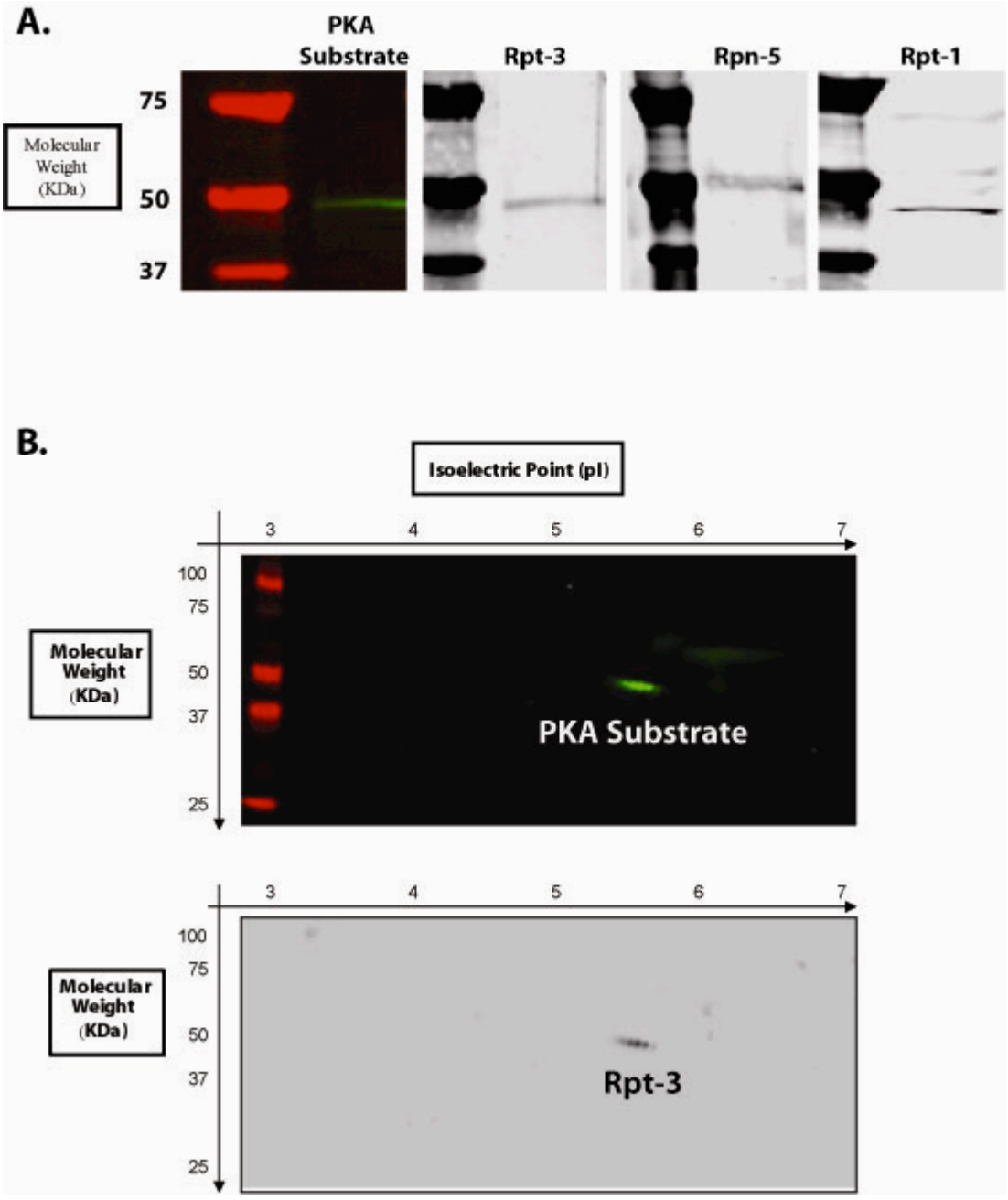

Figure 11. Detection of PKA-dependent phosphorylation of UPS subunits. A. Representative immunoblots of 15 µg of the purified 19S complex probed with an antibody against PKA-dependent phosphorylation that was subsequently stripped and reprobed for specific 19S subunits. **B.** Representative immunoblot of a 2-DE probed with an antibody against PKA-dependent phosphorylation and subsequently stripped and reprobed with a Rpt-3 specific antibody. The spots on a SYPRO RUBY stained 2DE corresponding to location of the Rpt-3 and PKA antibody detection were gel excised and found to be mitochondrial Atp5b ATP synthase subunit beta.

Figure 12

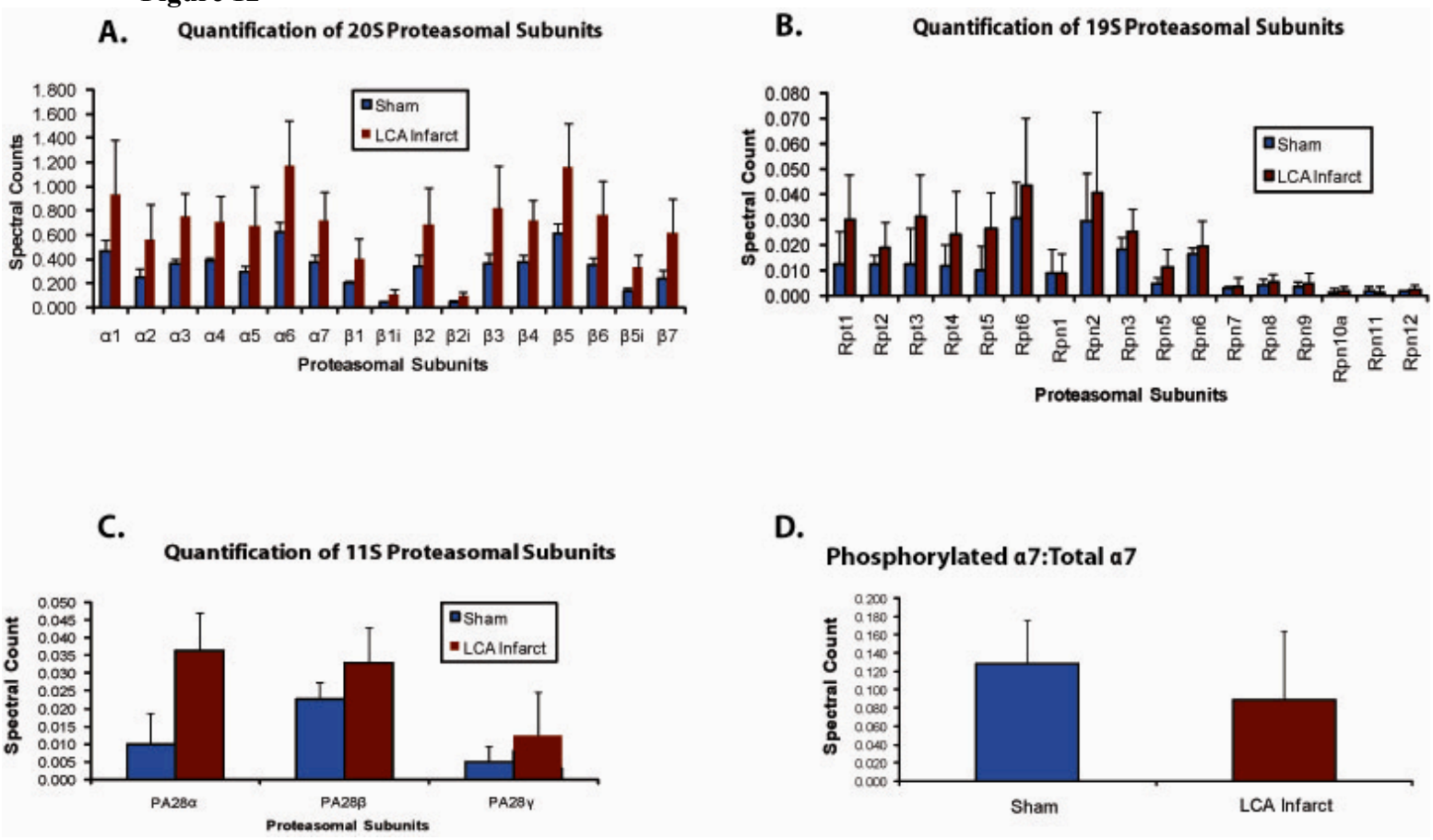

Figure 12. LC/MS/MS proteomic profiling of UPS subunits and phosphor analysis of α-7 subunit in sham vs. infarct mice. A. Quantification of the spectral counts obtained from LC/MS/MS analysis for subunits from the 20S complex in Sham vs. LCA infarct tissue relative to TnI as a control (n=3 per group). Statistical analysis revealed no significant difference in any of the subunits within the 20S complex in Sham vs. infarcted mice. **B.** LC/MS/MS analysis for subunits of the 19S complex in Sham vs. LCA infarct tissue standardized to actin as a control (n=3 per group) demonstrated no significant difference subunit expression within the 19S complex. **C.** Quantification of the spectral counts obtained from LC/MS/MS analysis for subunits from the 11S complex in Sham vs. LCA infarct relative to TnI as a control (n=3 per group). Statistical comparison showed there to be no difference in subunit expression between the groups in question. **D.** Quantification of phosphorylated α7 based on LC/MS/MS spectral counts expressed as a ratio to total α7 in Sham vs. LCA infarct. Statistical analysis showed no significant difference in phosphorylation of α7 between the two groups (p= 0.488).